Effects of management and pore characteristics on organic matter composition of macroaggregates; evidence from imaging and approaches for characterization of organic matter

E.R. Toosi[a], A.N. Kravchenko[a], J. Mao[b], M.Y. Quigley[a] & M.L. Rivers[c]

[a]*Department of Plant, Soil and Microbial Sciences, Michigan State University, East Lansing, MI 48823 USA,* [b]*Department of Chemistry and Biochemistry, Old Dominion University, Norfolk, VA 23529, USA, and* [c]*Center for Advanced Radiation Sources, The University of Chicago, Argonne National Lab, Argonne, IL 60439, USA.*

Correspondence: E.R. Toosi. Email: ertoosi@gmail.com

Running title: Pore characteristics and OM composition of macroaggregates

Summary

Macroaggregates are of interest because of their fast response to land management and their role in the loss or restoration of soil organic C (SOC). The study included two experiments. In *Experiment I*, we investigated the effect of long-term (27 years) land management on the chemical composition of organic matter (OM) of macroaggregates. Macroaggregates were sampled from topsoil under conventional cropping, cover cropping and natural succession systems. The OM of macroaggregates from conventional cropping was more decomposed than that of cover cropping and especially natural succession, based on larger $\delta^{15}N$ values and decomposition indices determined by multiple magic-angle spinning nuclear magnetic resonance (^{13}C CP/MAS NMR) and Fourier transform infrared (FTIR) spectroscopy. Previous research at the sites studied suggested that this was mainly because of reduced diversity and activity of the decomposer community, change in nutrient stoichiometry from fertilization and contrasting formation pathways of macroaggregates in conventional cropping compared to cover cropping and specifically, natural succession. In *Experiment II*, we investigated the relation between OM composition and pore characteristics of macroaggregates. Macroaggregates from the natural succession system only were studied. We determined 3-D pore-size distribution of macroaggregates with X-ray microtomography, for which we cut the macroaggregates into sections that had contrasting dominant pore sizes. Then, we characterized the OM of macroaggregate sections with FTIR and $\delta^{15}N$ methods. The results showed that within a macroaggregate, the OM was less decomposed in areas where the small (13–32 μm) or large (136–260 μm) pores were abundant. This was attributed to the role of large pores in supplying fresh OM, and small pores in the effective protection of OM in macroaggregates. Previous research at the site studied had shown increased abundance of large and small intra-aggregate pores following

adoption of less intensive management systems. It appears that land management can alter the OM composition of macroaggregates, partly by the regulation of OM turnover at intra-aggregate scale.

Keywords: pore size, aggregate porosity, FTIR, X-ray microtomography, ^{13}C CP/MAS NMR, land management, conventional cropping, cover cropping, natural succession

Highlights

• OM and pore characteristics were studied in soil macroaggregates under different land management.

• Long-term intensive land management increased degree of OM decomposition in macroaggregates.

• Abundance of <32 μm and >136 μm pores were positively related to less decomposed OM.

• Land management may affect rate of SOM turnover by changing intra-aggregate pore-size distribution.

Introduction

The composition of soil organic matter (SOM) controls nutrient cycling, rate of SOC turnover and the response of soil to an increase in temperature (von Lüetzow & Kögel-Knabner, 2010; Erhagen *et al*., 2013). In contrast to the widely studied effects of changes in land management on SOC stocks, few studies have investigated these effects on the composition of SOM and their findings have been inconsistent (Mahieu *et al*., 1999; Panettieri *et al*., 2013). On the other hand, compared to the whole soil, OM turnover is faster in macroaggregates (>250 μm) and they have a greater abundance of undecomposed plant materials (Tisdall & Oades, 1982). Therefore, it has been suggested that compared to the whole soil, macroaggregates might reflect better changes in SOM composition that result from management (Panettieri *et al*., 2013).

The role of macroaggregates in the protection of SOM has been well documented. The current understanding of aggregate dynamics is based on studying the aggregate matrix with destructive techniques such as physical separation and isolation. Transformations of OM inside macroaggregates, however, are largely regulated by pore characteristics, an underappreciated property of aggregates (Elliot *et al*., 1980). Research on pore characteristics in intact macroaggregates has been hampered by methodological difficulties. Therefore, the use of emerging non-destructive approaches such as 'imaging' as a complementary approach is essential to examine aggregate 'pore hierarchy' (Kravchenko *et al*., 2014; Six & Paustian, 2014).

Physical protection of OM within macroaggregates is attributed in part to reduced accessibility of intra-aggregate OM to decomposers. Accessibility ultimately results from the presence and characteristics of pores (Vogel *et al*., 2015) that indirectly regulate OM turnover inside aggregates through fluxes of gases and solutes (including substrate). The fluxes control key mechanisms involved in OM dynamics within aggregates such as (i) activity of micro and meso fauna (Brown *et al*., 2000; Strong *et al*., 2004), (ii) activity and community composition of microorganisms (Brown *et al*., 2000) and also (iii) movement of exo-enzymes (Smucker *et al*., 2007). Pores also create microhabitats for microbes against predators (Elliot *et al*., 1980; Ruamps *et al*., 2011). A few studies have demonstrated quantitative relations between the abundance of specific pore sizes and C dynamics. For example, accelerated decomposition has been shown to occur in the presence of pores of 15–60 μm (Strong *et al*., 2004; Ruamps *et al*., 2011). Therefore, we can postulate that within a macroaggregate, abundance of specific size classes of pores affects OM decomposition and thus its chemistry.

In this study, we investigated (i) the effect of land management on OM composition of macroaggregates (*Experiment I*) and (ii) searched for possible relations between the abundance of size of intra-aggregate pores with the degree of OM decomposition (*Experiment II*). In *Experiment I*, we compared OM characteristics in macroaggregates from soil under 26 years of contrasting management. We characterized the OM of macroaggregates with multiple magic-angle spinning nuclear magnetic resonance (^{13}C CP/MAS NMR) and Fourier transform infrared (FTIR) spectroscopy and $\delta^{15}N$ to determine whether long-term establishment of less intensive management has resulted in less decomposed OM in macroaggregates than with conventional cropping.

In *Experiment II*, we combined 'SOM characterization' and 'imaging' approaches to assess possible relations quantitatively between the abundance of intra-aggregate pore sizes and degree of OM decomposition. We hypothesized that within a macroaggregate, more medium-size pores (30–70 μm) are associated with more decomposed OM, whereas more small pores (<30 μm) are associated with less decomposed OM. To test the hypothesis, we compared OM characteristics of macroaggregate sections within the 13–260 μm range of pore size. The X-ray computed microtomography (X-ray μ-CT) was used to obtain 3-D images of intact macroaggregates. After information on pore characteristics was obtained, we sliced each macroaggregate into sections based on dominant pore-size distribution and characterized the OM properties of each section with $\delta^{15}N$ and FTIR techniques. To the best of our knowledge, differences in OM composition at the intra-aggregate scale and as a function of pore size have not been investigated previously.

Materials and Methods

Site and soil sampling

The soil sampling was conducted at the Long-Term Ecological Research (LTER) site at Kellogg Biological Station (KBS, 85˚ 24´W, 42˚ 24´N) established in 1989 in southwest Michigan, US. Detailed description of the LTER experiment can be found at www.lter.kbs.msu.edu. Samples were selected from soil under a gradient of land management intensity with conventional cropping > cover cropping > natural succession. Both conventional and cover cropping included maize (*Zea mays* L.), soya beans (*Glycine max* L.) and wheat (*Triticum aestivum* L.) in the rotation. The cover cropping system also had leguminous winter cover crops such as rye (*Secale cereal* L.) and clover (*Trifolium pratense* L.) (Table 1). The natural succession had a diverse range of mainly herbaceous plant species. Unlike conventional cropping, the cover cropping and natural succession did not receive manure or fertilizer and had vegetation all year. There was no cropping or cultivation in plots under natural succession, but the plots were burned annually in spring to prevent tree growth.

The soil was a mixed, mesic Typic Hapludalf (Mokma & Doolittle, 1993). The soil texture was fine loam and the soil pH was 6.4 for the sampling depth of 15 cm. Sampling was done in February 2012, following maize in the rotation of both conventional and cover cropping. Soil samples were taken from adjacent experimental plots at three randomly selected sampling sites located ~30 m apart within each plot. At each sampling site an intact cube of soil (15 cm × 15 cm × 15 cm) was extracted with a spade. Sampling sites were regarded as replicates in the subsequent experiments and data analyses. The decision to use sampling sites from adjacent experimental plots only limits the scope for inference from our study to the soil conditions of the small area that was sampled. Unfortunately, the time-consuming and expensive nature of FTIR, NMR and computed tomography measurements limited the number of samples that we could process in this study. Our approach of close spatial proximity with adjacent experimental plots reduced inherent soil variation in the sample to achieve more accurate comparisons among the management systems.

Field-moist samples were air-dried, passed through 4- and 6-mm sieves where macroaggregates of 4–6 mm were collected. Aggregate selection started by picking the initial group of aggregates randomly from the sieve. These aggregates were then inspected visually and only those that did not appear excessively fragile and would survive further experimentation, i.e. scanning and cutting, were selected for the analyses.

Experiments

The study included two experiments. In *Experiment I,* we investigated OM characteristics of macroaggregates from soil under the three land management systems. In *Experiment II*, we explored associations between intra-aggregate OM characteristics and pore characteristics. Macroaggregates from soil of the natural succession system only were used for *Experiment II*.

Two subsamples (from each of the three sampling points) of macroaggregates from the soil under natural succession were created, and one was used for each of the two experiments. Aggregate imaging and aggregate section analysis are time-consuming and labour intensive, therefore, it was not feasible to do these analyses for aggregates from the other management systems. The macroaggregates used for *Experiment II* included at least one macroaggregate from each sampling site. Selection of the native succession system to be used in *Experiment II* was based on previous research that showed this system resulted in greater macroaggregate stability and abundance (Gandy & Robertson, 2007), and there were strong relations between pores and soil carbon within the 4–6 mm macroaggregates (Ananyeva *et al*., 2013).

Experiment I

From the macroaggregates of each sampled site (three sites per plot), an adequate number of macroaggregates (~50 g) were weighed and finely ground (<200 µm) with a ballmill. Subsamples of the ground macroaggregates were used for the analysis of soil C, N, ^{15}N natural abundance ($\delta^{15}N$), FTIR and ^{13}C CP/MAS NMR. Ground macroaggregates were weighed (55–65 mg) into tin capsules and analysed for C, N and $\delta^{15}N$ at the Stable Isotope facility at the University of California, Davis with a GmbH Elementar analyzer (Hanau, Germany) interfaced to a PDZ Europa 20-20 IRMS (Sercon Ltd., Crewe, UK). The use of $\delta^{15}N$ was based on the assumption that it is positively related to the degree of decomposition of SOM). Preferential discrimination of the lighter N isotope (^{14}N) occurs during decomposition of plant residue, resulting in ^{15}N enrichment of SOM compared to the initial litter ((Kramer *et al*., 2003).

For spectroscopic characterization, the soil samples were treated with hydrofluoric acid (HF) to obtain high resolution spectra). Briefly, 15 g of each sample (finely ground aggregates) was mixed with 150 ml 5% HF and the suspension was shaken overnight. The suspension was then centrifuged at 5000 ***g*** for 15 minutes and the supernatant was discarded. The procedure was repeated four times. Thereafter, the HF was removed from the residue by mixing it with 100 ml deionized water and the suspension was shaken for 2 hours. The suspension was centrifuged as above. The residue was dried under a ventilated hood and used for further analysis. For the ^{13}C CP/MAS NMR analysis of each management system, the three replicates (5 g of each) of ground macroaggregates were pooled together and treated with HF as described above. Therefore, there was one composite sample for each management type.

For FTIR analysis, 100 mg of a mixture composed on 99% HF treated sample and 1% potassium bromide (KBr) was used to make a KBr pellet. The mixture was placed into the pellet holder and gradually compressed to a final 69 000 KPa for 2 minutes. The spectra were recorded with a Galaxy 3025 FTIR spectrophotometer (Mattson Instruments Inc., Madison, WI, USA) in the range 4000–600 cm^{-1} in absorbance mode while obtaining 32 scans at 4 cm^{-1} resolution. A pure KBr pellet was used for the background subtraction before analysing the sample and after every 10 samples. Before the acquisition of spectra, each pellet was held in the vacuum chamber for 5 minutes. Two spectra were recorded for each sample. After the first spectrum was acquired, the pellet was reversed, rotated 90° and the second spectrum recorded. The FTIR indices (below) were calculated for each spectrum and an average of the two was reported for the sample.

We selected the peak height approach for quantitative comparison of the FTIR spectra among the samples. The peaks included a peak at 1423 cm^{-1} (CH_3 deformation and CH_2 bending), peaks at 1648 and 1630 cm^{-1} (aromatic C=C and C=O vibrations), peak at 1724 cm^{-1} (C=O stretching of COOH), peak at 2930 cm^{-1} (asymmetric stretching of C–H in CH_2) and a peak at 1510 cm^{-1}

(secondary amide (C-N-C)) (Baes & Bloom, 1989; Inbar *et al*. 1989; Haberhauer *et al*., 1998). The ratio of two representative peaks was used to represent the decomposition status of SOM (Figure 1). Four indices were derived from the peaks i.e. Index 1: 1648/1423 (relative aromatic to aliphatic intensity), Index 2: 1648/1724 (relative aromatic to O functionality of carboxyl), Index 3: 2924/1724 (relative aliphatic C functionality to O functionality) and Index 4: 1630/1510 (relative carboxyl and aromatic to amide II). All the indices have been shown to increase with increasing decomposition status of OM and are positively correlated with measures of soil quality such as potassium permanganate-oxidizable organic C, dehydrogenase activity, water stable aggregates and water extractable organic OM (Inbar *et al*. 1989; Haberhauer *et al*., 1998; Veum *et al*., 2013).

The solid-state NMR analysis was performed on an Avance 400 spectrometer operating at a ^{13}C frequency of 100 MHz, with a 4-mm double-resonance probe head. The large-spinning speed multiple-cross polarization or magic angle spinning technique (multi CP/MAS) was applied to acquire quantitative ^{13}C NMR spectra. The spectra were measured at a spinning speed of 14 kHz. The 90° pulse lengths were 4 μs for ^{1}H and 4 μs for ^{13}C. All spectra were recorded with a Hahn echo generated by a 180° pulse with EXORCYCLE phase cycling applied to one rotation period (tz) after the end of cross polarization to achieve dead time-free detection (i.e. detection is initiated following sufficient dissipation of energy of the pulse). The increase in amplitude (ramp) of cross plarization was implemented with 11 steps of 0.1 ms duration and an increment in amplitude of 1% (90 to 100%). The recycle delays were 0.35 s. The duration of the repolarization period (tz) in multi CP was 0.3 s. The assigned regions were: alkyl carbon, 0–44 ppm; OCH_3/NCH, 44–61 ppm, O-alkyl, 61–93 ppm; anomerics, 93–113 ppm; aromatics, 113–142; aromatic C–O, 142–162 ppm; COO/N-C=O, 162–182 ppm; ketone and aldehyde, 186–220 ppm. The ratio of alkyl C to O-alkyl

C, aromatic C to O-alky C and alkyl C plus aromatic C to O alkyl C were determined as indicators that are positively related to the degree of OM decomposition.

Experiment II

For *Experiment II*, we used four randomly selected macroaggregates from the native succession vegetation land use. Each aggregate was subjected to X-ray μ-CT scanning followed by image analyses and pore characterization. The 3-D images of each aggregate were examined to identify the sections within the aggregates with contrasting pore characteristics, for example, sections with primarily small (13–30 μm) pores and those with large (115–260 μm) pores. Based on examination of the image, an individual cutting scheme was devised for each aggregate with 8–11 sections (11 to 56 mg) identified for each aggregate. Following the scheme, each aggregate was cut into sections both virtually, i.e. the aggregate's 3-D image, and physically, i.e. the actual aggregate. Cutting was done with a scalpel under 30-times magnification. Our aim was to have sections with somewhat contrasting pore characteristics, for which the 3-D image of each aggregate was examined visually. If a sizeable area (minimum 2 mm × 2 mm × 2 mm) with no visible large pores or with large visible pores was identified within the aggregate, we tried to ensure the area would be within the same cut section. It was not possible to cut soil aggregates on a fixed lattice, because of their irregular shapes and the inclusions of large sand grains. Because of difficulties with matching the 3-D pore map of aggregates and the slicing procedure, we were partially successful only in achieving contrasting pore characteristics of the sections. Furthermore, because of the small amount of soil in each section and destructive nature of the characterization methods, the soil of each section was subjected to either FTIR or δ^{15}N analysis. From each aggregate, we used 3–4 sections for FTIR and 3–8 sections for δ^{15}N analysis. We used the larger sections for FTIR analysis to ensure adequate C content of the sample after HF treatment. The four macroaggregates provided 12 sections for FTIR and 22 sections for $\delta^{15}N$. Because of the small size of sections and therefore their small C content, we were unable to do the NMR analysis.

For the FTIR analysis, we developed a sample preparation procedure (below) that enabled characterization of soil samples within the range of 25–56 mg samples. Each section was transferred into a 2 ml microtube and 5% HF was added to the tube in proportion to the mass of the aggregate section (at the ratio of 1 g in 10 ml). The suspensions were shaken with a Vortex (Corning LSE, Corning Inc., MA, USA) for 4 hours followed by centrifugation. The supernatant was discarded. The procedure was repeated four times. Then the residue was washed with deionized water, centrifuged and dried as mentioned above. The residue was mixed with KBr (99% + 1%, respectively) and the mixture was used for the KBr pellet. The FTIR sample analysis and calculations of decomposition indices were done as described above for the whole macroaggregates.

X-ray μ-CT scanning and image analyses

The macroaggregates were scanned on the bending magnet beam line, station 13-BM-D of the GeoSoilEnviron CARS at the Advanced Photon Source, Argonne National Laboratory, Argonne, IL, USA. Details of instrumental configuration and image processing are given in Rivers & Wang (2006) and Kravchenko *et al*. (2014). The image data were recorded with the Si double crystal monochromator with a 55-m distance from sample to source. Data were combined into a 3-D image of 520 slices with 696 × 696 pixels per slice. The voxel size was 13 μm × 13 μm × 13 μm. The data were preprocessed by removing ring artifacts, corrected for dark current (the signal obtained in the absence of any X-rays) and flat field (the signal obtained with the X-rays on, but without a sample), and reconstructed with the GridRec fast Fourier transform reconstruction algorithm.

Classification of image voxels into pore or solid material was done with indicator kriging (Oh & Lindquist, 1999). The benefit of indicator kriging is that thresholds are set so that not only the grey-scale values of the voxel itself but also those of the surrounding voxels are considered. Four pore characteristics were derived from the images: (i) total porosity, (ii) image-based porosity, (iii) pores below image resolution and (iv) size distributions of visible pores. Total porosity was calculated from the weight and volume data of each aggregate (assuming a bulk density of 2.6 g cm^{-3}) and represent pores of all sizes. Image-based porosity was assessed as the percentage of pores visible at the image resolution (>13 μm). Percentage of pores below image resolution, i.e. pores < 13 μm, was calculated as the difference between total and the image-based porosity. Pore-size distributions were obtained by the 'burn number distribution approach' (Lindquist *et al*., 2000). This approach identifies the medial axis of pores within the images by a series of simultaneous 'burn' steps: the first step starts at the pore voxels adjacent to the solid voxels and assigns them a burn number of 1, the next step processes the pore voxels adjacent to burn number 1 voxels and assigns them a burn number of 2, and so on. The process continues until the burn steps from two or more directions enter the same voxel, which is the voxel retained as a medial axis voxel. Average size distribution values from the macroaggregate sections studied are shown in Figure S1.

Intra-aggregate particulate organic matter (POM) was determined with the procedure developed by Kravchenko *et al* (2014). In brief, POM particles were selected from the images based on size, shape and greyscale values from the image, followed by discriminant classification of the data with statistical and geostatistical parameters from the greyscale values of POM particles. The parameters we used in this study were the mean, standard deviation, skewness, kurtosis, spatial correlation range and nugget-to-sill ratio. The approach requires the user to identify the training data set of POM particles and artifacts, on the basis of which the discrimination of the rest of the image is conducted. Most of the image analyses used tools from 301 ImageJ (Rasband, 1997 to 2012) and its plug-in tools 3-D Viewer, whereas indicator kriging segmentation and pore-size distributions were implemented in 3DMA-Rock software (Lindquist *et al*., 2000).

Statistical analysis

Comparisons of all data (except ^{13}C CP/MAS NMR) for the three land management systems from *Experiment I* were made by the analysis of variance in a completely randomized design setting, with 3 treatments and 3 replicates per treatment. The normality of residuals and assumptions of the homogeneity of variances were checked for all variables and were acceptable. There were no outliers in the data. The analyses were performed with the PROC MIXED procedure of SAS (Version 9.4, SAS Institute, 2012).

The associations of FTIR derived indices, FTIR derived regions and $\delta^{15}N$ with intra-aggregate pore characteristics in *Experiment II* were assessed with simple and multiple regression analyses using the PROC CORR and PROC REG procedures of SAS.

Results

The organic C concentrations of macroaggregates from the natural succession and cover cropping systems were 1.9 and 1.4 times greater, respectively, than that of conventional cropping (Tables 2 and 3). Similarly, total N (TN) concentrations were 1.7 and 1.4 times greater in the natural succession and cover cropping, respectively, than that of conventional cropping. The $\delta^{15}N$ was greater for macroaggregates from conventional cropping than for those of the other land uses, but there was no statistically significant difference between macroaggregates from the natural succession and cover cropping. (Tables 2 and 3).

The FTIR spectra of HF treated samples (Figures 1 and S2) had distinct peaks in the aliphatic region (3000–2800 cm^{-1}), aromatic region (1650–1630 cm^{-1}) and the carboxyl shoulder at 1720±5 cm^{-1}. The decomposition indices (i.e. Index 1 to 4) indicated differences in OM characteristics of macroaggregates among the different management systems; the indices were significantly larger for macroaggregates from conventional cropping than from cover cropping or natural succession (Figure 2 and Table 3).

In the ^{13}C CP/MAS NMR spectra (Supporting Information, Figure S3) the peak around 30 ppm was attributed to long-chain polymethylene, and that around 55 ppm to both OCH_3 and NCH groups. The second dominant band around 72 ppm represented OCH_2, probably that of carbohydrates. The small shoulder around 105 ppm was the signal of O–C–O anomers of carbohydrates. The signals of aromatics appeared around 130 ppm and those of aromatic C–O, such as phenolics, were present as a shoulder around 150 ppm. The band around 172 ppm was attributed to COO/N–C=O groups, but signals for ketones and aldehydes (around 190) ppm were barely above the baseline. The relative proportions of different functional groups based on integration of the multi CP/MAS spectra are given in Table 4. The proportional intensity of O-Alkyl (mainly representative of polysaccharides) followed natural succession> cover cropping > conventional cropping. In contrast, the proportion of aromatic C and aromatic C–O were larger for macroaggregates from conventional cropping than from the other two management systems.

Accordingly, the ^{13}C CP/MAS NMR-based OM decomposition indices showed a consistent pattern with management intensity; alkyl C/O-alkyl C, aromatic C/O-alkyl C and alkyl C+aromatic/O-alkyl C of macroaggregates followed the pattern conventional cropping > cover cropping > natural succession.

Experiment II

The FTIR-derived decomposition indices and $\delta^{15}N$ values (Table S1) were correlated significantly with several image-based pore characteristics (Table 5). In addition, total porosity of macroaggregates was positively correlated with SOC and TN, but was negatively correlated with $\delta^{15}N$ and Index 2. Percentage of pores <13 μm and >13 μm image resolution were strongly and negatively correlated with Index 2 and Index 3 values, respectively. Pores 13–32 μm in size were strongly negatively correlated with Index 1 and 4 values. The presence of large pores (>136 μm) was negatively correlated with Indices 2, 3 and 4 (Table 5) and presence of the maximum pore size observed was negatively correlated (R^2 = 0.35 to 0.45) with all four decomposition indices (Figure 3). The presence of large pores (>136 μm) was also negatively correlated with $\delta^{15}N$ values.

Multiple linear regression models with 13–32 μm and >136 μm pores as independent variables explained as much as 51–75% of the intra-aggregate variation in values of FTIR Indices 1, 2 and 4 (Table 6). The multiple regression models were significant at values of 0.1 for Index 3 and $\delta^{15}N$. Pores of 13–32 μm and >136 μm had negative regression coefficients for all models.

Discussion

Experiment I: OM characteristics of macroaggregates under contrasting management systems

The OM of macroaggregates from long-term less intensive management systems was less decomposed. Compared to the cover cropping and in particular natural succession, the OM of macroaggregates from conventional cropping had larger $\delta^{15}N$ (Tables 2 and 3) and greater decomposition indices based on FTIR (Figure 2) and ^{13}C CP/MAS NMR (Table 4). Given that the soil and climatic conditions were almost identical at the site studied, long-term interactions between litter input, intensity of disturbance, stoichiometry of nutrients and composition of the decomposer community appear to be the primary factors that have affected OM chemistry of macroaggregates.

Primary controlling factors in OM composition of macroaggregates

Soil disturbance enhances the rate of SOM decomposition, mainly because of aggregate disruption and enhanced oxidation (Tisdall & Oades, 1982; Toosi, *et al*., 2012, 2014). However, the intensity of mechanical disturbance was greater in the cover cropping than conventional cropping (Table 1). Litter quality, specifically from belowground sources might have contributed to the OM composition of macroaggregates. Diverse litter input in the natural succession contrasts with that under the other two types of management, where maize, soya beans and wheat were the major source of litter input (the biomass from cover crop was ~ 14% of the main crop). The strong effect of initial litter quality on SOM composition, however, diminishes over time (Mahieu *et al*., 1999). Together, it seems that litter input and mechanical disturbance do not explain adequately the differences in OM composition of macroaggregates under the management systems studied. This can be explained by the effect of fertilizers, aggregation dynamics and contrasting compositions of the decomposer community.

Previous research at the site studied indicated that cover cropping and natural succession managements diversified soil faunal and microbial community (e.g. Smith *et al*., 2008; Lauber *et al*., 2013;). On the other hand, intensive management often results in greater bacterial abundance and activity of oxidative enzymes, i.e. enzymes primarily responsible for poor quality substrate (Bradford *et al*., 2002; McDaniel *et al*., 2014). Therefore, the more advanced degree of OM decomposition in macroaggregates from conventional cropping than for the other two management systems might partly result from its less diverse decomposer community that has a greater capability to decompose less favourable substrates, leaving behind more decomposed compounds.

Fertilization might also have contributed to contrasting OM chemistry of macroaggregates. Long-term supply of N and P can change the broad C:N:P of soil towards a narrower elemental stoichiometry. This enhances microbial 'mining' for C and results in further decomposition of SOM (Cleveland & Townsend, 2006; Bradford *et al*., 2008).

Pathways of macroaggregate formation are affected by management i.e. primarily physicochemical-based formation in the conventional cropping and biologically-based aggregation in the cover cropping and natural succession (Smucker *et al*., 2007; Kravchenko *et al*., 2014). Macroaggregates formed under the cover cropping and natural succession had slower turnover rates (Grandy & Robertson, 2007), greater abundance of fine roots and associated mycorrhizae, and more diverse pore characteristics (that contribute specifically to protect fresh OM) than those under conventional cropping (Kravchenko *et al*., 2011; Ananyeva *et al*., 2013). These together might have resulted in more of the less decomposed OM in macroaggregates under the less intensive management.

Experiment II: OM characteristics in relation to intra-aggregate pores

There were negative relations between the proportion of large (>136 μm) and small (13–32 μm) pores with δ^{15}N and FTIR-derived decomposition indices of aggregate sections (Figure 3, Tables 5 and 6). This suggests that abundance of large and small intra-aggregate pores of the macroaggregates studied were associated with less decomposed OM. Contrary to our expectation, abundance of medium size pores (32–136 μm) was not related to the OM characteristics examined.

Large (>136 μm) and small (13–32 μm) pores explained 50–75% of variation in the degree of OM decomposition in the macroaggregates studied. Strong negative correlations ($P<0.05$) between (i) abundance of large pores (>136 μm) and (ii) maximum pore size with δ^{15}N and decomposition indices of macroaggregate sections reflected the function of large pores of these macroaggregates as avenues of fresh OM inputs. Previous research at the site studied indicated that biological processes strongly contribute to the formation of macroaggregates in the natural succession (Kravchenko *et al*., 2013). This is partly because of large faunal and microbial activity in the soil studied (e.g. Smith *et al*., 2008), but also because of the lack of mechanical disturbance, reduced drying–wetting cycles (from year-round vegetation) and presence of diverse rooting systems. The large pores, typically with round shapes represent 'biopores' (Figure 4), contain either the remains of fine roots or are shaped specifically by mesofauna (Coleman & Wall, 2007). Therefore, the reverse relation between less decomposed OM and large intra-aggregate pores is attributed specifically to fresh OM inputs such as root exudates, remains of fine roots and their associated mycorrhizae, and excretions and mucilage of the burrowing fauna and their associated microflora.

The OM of macroaggregate sections with abundance of small (13–32 μm) pores appeared to be less decomposed. This is consistent with the smaller rate of mineralization reported of various substrates where pores are <1–100 μm (Shaw *et al*., 2002; Ruamps *et al*., 2011). The small pores effectively protect OM because (i) the proportionally large surface area of small pores enhance OM protection through processes of binding by minerals (Kaiser & Guggenberger, 2003) and (ii) OM in small pores is spatially inaccessible or poorly accessible for microbes and exo-enzymes (Smucker *et al*., 2007).

Previous research at the site studied showed that macroaggregates with stronger biological origin (natural succession) have a greater proportion of pores >100 µm than those under the intensive management, (Wang *et al*., 2012). Macroaggregates under natural succession also had larger C and N concentrations, which was consistent with the results of Ananyeva *et al*. (2013). In addition, their overall degree of OM decomposition was less than that in the macroaggregates under conventional cropping. Together, these results suggest that greater total porosity and more large (>136 µm) and small (13–32 µm) pores in macroaggregates under the less intensive system might have resulted in a slower rate of OM turnover inside macroaggregates, which contributed to their larger C content.

Management intensity and soil macroaggregate C, combining large and small scales

Long-term establishment of cover cropping or natural succession enhanced soil C within the A/Ap horizon (0.6±0.1 and 1.3±0.1 kg C m^{-2}, respectively) (Syswerda *et al*., 2011). This was attributed primarily to a slower rate of turnover and more macroaggregates under the less intensive systems (Grandy & Robertson, 2007). Grandy & Robertson (2007) also reported greater C contents in macroaggregates under the less intensive management systems, which was consistent with our results. It appears that the abundance and stability of macroaggregates and their larger C concentration under the less intensive management systems have contributed to the larger SOM content in the topsoil. On the other hand, the increased C concentration, and the overall smaller degree of OM decomposition of macroaggregates under the less intensive management systems accords with greater pore heterogeneity of these macroaggregates (i.e. greater abundance of large and small pores) (Wang *et al*., 2012; Kravchenko *et al*., 2011 and 2013). This suggests that an increase or decrease in topsoil C following a long-term change in management partly underlies changes in intra-aggregate pore characteristics, which are closely associated with the content and chemistry of carbon in macroaggregates (Figure 5).

Conclusions

Land management affects macroaggregates namely by mechanical disturbance and pathways of macroaggregate formation. In *Experiment I*, we observed that in a soil that has been under contrasting management systems for 26 years, the overall OM decomposition of macroaggregates was: conventional cropping > cover cropping ≥ natural succession. Greater abundance and stability of macroaggregates under less intensive management can often predict the accumulation of SOC in topsoil. We propose that given the role of macroaggregates in the protection of SOM and the faster rate of OM turnover in macroaggregates than in bulk soil, changes in the OM composition of macroaggregates might provide an early indication of changes in SOM chemistry in the longer term. In *Experiment II*, we showed that in macroaggregates under natural succession the OM was less decomposed within a macroaggregate in the areas with greater abundance of small (13–32 μm) or large (136–260 μm) pores. Macroaggregates under the less intensive management systems have greater abundance of both large and small pores. Quantitative assessment of interactions between pores and rate of OM decomposition is lacking. Nevertheless, our results suggest that land management might indirectly affect OM turnover at the intra-aggregate scale by regulating interactions between pore-size distribution and the rate of OM decomposition.

Supporting Information

The following supporting information is available in the online version of this paper:

List of plant species in the natural succession system: https://lter.kbs.msu.edu/datatables/154

Figure S1. Pore-size distribution for each of the macroaggregate sections obtained from X-ray μCT images.

Figure S2. The FTIR spectra for the macroaggregates from conventional cropping, cover cropping and natural succession.

Figure S3. The multi CP/MAS ^{13}C-NMR spectra of macroaggregates from conventional cropping, cover cropping, and natural succession.

Table S1. Values of FTIR-derived decomposition indices and δ^{13}N for each of the macroaggregate sections.

Acknowledgments

Support for this research was provided in part by the United States Department of Agriculture (USDA) National Institute of Food and Agriculture (NIFA) award No. 2011-68002-301907 Cropping Systems Coordinated Agricultural Project (SCCAP); by the U.S. National Science Foundation Long-Term Ecological Research (LTER) Programme at the Kellogg Biological Station (DEB 1027253); by Kellogg Biological Station; by Michigan State University's "Project GREEEN" Program and by Michigan State University's "Discretionary Fund Initiative" Program. Special thanks to Dr. Kathryn Severin for providing access to the FTIR facility. The authors greatly appreciate the constructive comments provided by the reviewers and Professor M. Oliver.

References

Ananyeva, K., Wang, W., Smucker, A.J.M., Rivers, M.L. & Kravchenko, A.N. 2013. Can intra aggregate pore structures affect the aggregate's effectiveness in protecting carbon? *Soil Biology & Biochemistry*, **57**, 868–875.

Baes, A.U. & Bloom, P.R. 1989. Diffuse reflectance and transmission Fourier transform infrared (DRIFT) spectroscopy of humic and fulvic acids. *Soil Science Society of America Journal*, **53**, 695–700.

Bradford, M.A., Tordoff, G.M., Eggers, T., Jones, T.H. & Newington, J.E. 2002. Microbiota, fauna, and mesh size interactions in litter decomposition. *Oikos*, **99**, 317–323.

Bradford, M.A., Fierer, N. & Reynolds, J.F. 2008. Soil carbon stocks in experimental mesocosms are dependent on the rate of labile carbon, nitrogen and phosphorus inputs to soils. *Functional Ecology*, **22**, 964–974.

Brown, G.G., Barois, I. & Lavelle, P. 2000. Regulation of soil organic matter dynamics and microbial activity in the drilosphere and the role of interactions with other edaphic functional domains. *European Journal of Soil Biology*, **36**, 177−198.

Cleveland, C.C. & Townsend, A.R. 2006. Nutrient additions to a tropical rain forest drive substantial soil carbon dioxide losses to the atmosphere. *Proceedings of the National Academy of Sciences of the United States of America*, **103**, 10316–10321.

Coleman, D.C. & Wall, D.H. 2007. Fauna: the engine for microbial activity and transport. In: *Soil Microbiology, Ecology and Biochemistry*, Third Edition (ed. E.A. Paul), pp. 163–190. Academic Press, Burlington, VT, USA.

Elliott, E.T., Anderson, R.V., Coleman, D.C. & Cole, C.V. 1980. Habitable pore space and microbial trophic interactions. *Oikos*, **35**, 327–335.

Erhagen, B., Oquist, M. Sparrman, T., Haei, M., Ilstedt, U., Hedenstrom, M. *et al*. 2013. Temperature response of litter and soil organic matter decomposition is determined by chemical composition of organic material. *Global Change Biology*, **19**, 3858–3871.

Grandy, S. & Robertson, P. 2007. Land-use intensity effects on soil organic carbon accumulation rates and mechanisms. *Ecosystems*, **10**, 58–73.

Haberhauer, G., Rafferty, B., Strebl, F. & Gerzabek, M.H. 1998. Comparison of the composition of forest soil litter derived from three different sites at various decompositional stages using FTIR spectroscopy. *Geoderma*, **83**, 33I–342.

Inbar, Y., Chen, Y. & Hadar, Y. 1989. Solid-state carbon 13 nuclear magnetic resonance and infrared spectroscopy of composted organic matter. *Soil Science Society of America Journal*, **53**, 1695–1701.

Kaiser, K. & Guggenberger, G. 2003. Mineral surfaces and soil organic matter. *European Journal of Soil Science*, **54**, 219–236.

Kramer, M.G., Sollins, P., Sletten, R.S. & Swart, P.K. 2003. N isotope fractionation and measures of organic matter alteration during decomposition. *Ecology*, **84**, 21–25.

Kravchenko, A., Chun, H.C., Mazer, M., Wang, W., Rose, J.B., Smucker, A. *et al*. 2013. Relationships between intra-aggregate pore structures and distributions of Escherichia coli within soil macro-aggregates. *Applied Soil Ecology*, **63**, 134–142.

Kravchenko, A.N., Negassa, W.C., Guber, A.K. & Schmidt, S. 2014. New approach to measure soil particulate organic matter in intact samples using X-Ray computed microtomography. *Soil Science Society of America Journal*, **78**, 1177–1185.

Kravchenko, A.N., Wang, A.N.W., Smucker, A.J.M. & Rivers, M.L. 2011. Long-term differences in tillage and land use affect intra-aggregate pore heterogeneity. *Soil Science Society of America Journal*, **75**, 1658–1666.

Lauber, C.L., Ramirez, K.S., Aanderud, Z., Lennon, J. & Fierer, N. 2013. Temporal variability in soil microbial communities across land-use types. *ISME Journal*, **7**, 1641–1650.

Lindquist, W. B., Venkatarangan, A., Dunsmuir, J. & Wong, T. 2000. Pore and throat size distribution measured from synchrotron X-ray tomographic images of Fontainebleau sandstones. *Journal of Geophysical Research.*, **105B**, 21508–21528.

Mahieu, N., Powlson, D.S. & Randall, E.W. 1999. Statistical analysis of published carbon-13 CPMAS NMR spectra of soil organic matter. *Soil Science Society of America Journal*, **63**, 307–319.

McDaniel, M.D., Grandy, A.S., Tiemann, L.K. & Weintraub, M.N. 2014. Crop rotation complexity regulates the decomposition of high and low quality residues. *Soil Biology & Biochemistry*, **78**, 243–254.

Mokma, D.L. & J.A. Doolittle. 1993. Mapping some loamy Alfisols in southwestern Michigan using ground-penetrating radar. *Soil Survey Horizons*, **34**, 71–77.

Oh, W. & Lindquist, B. 1999. Image thresholding by indicator kriging. *IEEE Transactions on Pattern Analysis and Machine Intelligence*, **21**, 590–602.

Panettieri, M., Knicker, H., Berns, A.E., Murillo, J.M. & Madejon, E. 2013. Moldboard plowing effects on soil aggregation and soil organic matter quality assessed by ^{13}C CPMAS NMR and biochemical analyses. *Agriculture, Ecosystems & Environment*, **177**, 48–57.

Rasband, W.S. 1997–2012. *ImageJ*, U.S. National Institutes of Health, Bethesda, MD, USA. Available at http://rsb.info.nih.gov/ij/

Rivers, M.L. & Wang, Y. 2006. Recent developments in microtomography at GeoSoilEnviroCARS. In: *Proceedings of the SPIE, Developments in X-Ray Tomography V* (ed. U. Bones), **6318**, id. 63180J.

Ruamps, L.S., Nunan, N. & Chenu, C. 2011. Microbial biogeography at the soil pore scale. *Soil Biology & Biochemistry*, **43**, 280–286.

Shaw, L.J., Beaton, Y., Sousa, S., Glover, L.A., Killham, K. & Meharg, A.A. 2002. Mineralisation of 2,4-dichlorophenol and glucose placed into the same or different hydrological domains as a bacterial inoculant. *Soil Biology & Biochemistry*, **34**, 531–539.

Six, J. & Paustian, K. 2014. Aggregate-associated soil organic matter as an ecosystem property and a measurement tool. *Soil Biology & Biochemistry*, **68**, A4–A9.

Smith, R.G., McSwiney, C.P., Grandy, A.S., Suwanwaree, P., Snider, R.M. & Robertson, G.P. 2008. Diversity and abundance of earthworms across an agricultural land-use intensity gradient. *Soil & Tillage Research*, **100**, 83–88.

Smucker, A.J.M., Park, E.J., Dorner, J. & Horn, R. 2007. Soil Micropore Development and Contributions to Soluble Carbon Transport within Macroaggregates. *Vadose Zone Journal*, **6**, 282–290.

Strong, D.T., De Wever, H., Merckx, R. & Recous, S. 2004. Spatial location of carbon decomposition in the soil pore system. *European Journal of Soil Science*, **55**, 739–750.

Syswerda, S.P., Corbin, A.T., Mokma, D.L., Kravchenko, A.N. & Robertson, G.P. 2011. Agricultural Management and Soil Carbon Storage in Surface vs. Deep Layers. *Soil Science Society of America Journal*, **75**, 92–101.

Tisdall, J.M. & Oades, J.M. 1982. Organic matter and water-stable aggregates in soils. *Journal of Soil Science* **33**, 141–163.

Toosi, E.R., Schmidt, J.P. & Castellano, M.J. 2014. Land use and hydrologic flowpaths interact to affect dissolved organic matter and nitrate dynamics. *Biogeochemistry*, **120**, 89–104.

Toosi, E.R., Castellano, M.J., Jeremy, J.W. & Mitchell, D.C. 2012. Differences in soluble organic matter after 23 years of contrasting soil management. *Soil Science Society of America Journal*, **76**, 628–637.

Veum, K.S., Goyne, K.W., Kremer, R.J., Miles, R.J. & Sudduth, K.A. 2013. Biological indicators of soil quality and soil organic matter characteristics in an agricultural management continuum. *Biogeochemistry*, **117**, 81–99.

Vogel, L.E., Makowski, D., Garnier, P., Vieuble-Gonod, L., Coquet, Y., Raynaud, X. *et al*. 2015. Modeling the effect of soil meso- and macropores topology on the biodegradation of a soluble carbon substrate. *Advances in Water Resources*, **83**, 123-136.

von Lützow, M. & Kögel-Knabner, I. 2010. Response to the Concept paper: 'What is recalcitrant soil organic matter?' by Markus Kleber. *Environmental Chemistry*, **7**, 333–335.

Wang, W., Kravchenko, A.N., Smucker, A.J.M., Liang, W. & Rivers, M.L. 2012. Intra-aggregate pore characteristics: X-ray computed microtomography analysis. *Soil Science Society of America Journal*, **76**, 1159–1171.

Table 1. Summary of management practices and vegetation for the land management systems studied.

Land management	Tillage[1]	NPK source	Weeding	Vegetation[6]
Conventional cropping	Chisel & disk	Fertilizer[2]	Chemical & mechanical[3]	Maize–Soya beans–Wheat
Cover cropping	Chisel & disk	Cover crop[4]-N	Mechanical[5]	Corn (rye)–Soya beans–Wheat (clover)
Natural succession	None	None	None	Mixed annual and or perennial herbaceous and limited woody species

[1] Tillage depth: 0–25 cm

[2] The recommended rate based on soil testing and best management practices (50 kg ha^{-1} P_2O_5, 100 kg ha^{-1} K_2O; 135 kg ha^{-1} N).

[3] Mostly chemical, but infrequent mechanical weeding included (i.e. inter-row rotary cultivation)

[4] Cover crop included rye and clover.

[5] Inter-row rotary cultivation and hoeing, 4–8 times

[6] For the list of plant species in the natural succession system, see Supporting Information

Table 2. Selected properties of the organic matter of macroaggregates under different land management systems.

Land management	SOC	TN	C/N	$\delta^{15}N$
	%			‰
Conventional cropping	0.79	0.08	9.6	4.64
Cover cropping	1.13	0.12	9.6	3.76
Natural succession	1.51	0.14	10.9	3.18
Standard Error	0.089	0.008	0.119	0.209

Data are mean (n=3). For F and P values, see Table 3.

Table 3. The results of residual maximum likelihood (REML) analyses for soil properties (see Table 2) and FTIR decomposition indices (see Figure 2) for the completely randomized design of *Experiment I.* The fixed factor was land management. The *P*-values are less than 0.02 for all of the dependent variables.

		Soil Property							
		SOC		TN		C/N		$\delta^{15}N$	
Source	Degrees of freedom	Mean square	*F*	Mean square	*F*	Mean square	*F*	Mean square	*F*
Treatment	2								
Residual	6	0.024	16.3	0.000	12.1	0.043	42.7	0.132	12.3
Total	8								
		FTIR-based decomposition indices							
		Index 1		Index 2		Index 3		Index 4	
		Mean square	*F*	Mean square	*F*	Mean square	*F*	Mean square	*F*
Treatment	2								
Residual	6	0.003	13.2	0.000	16.8	0.001	8.1	0.001	8.8
Total	8								

Table 4. Percentages of major chemical shift regions and three variables to represent the status of SOM decomposition obtained from multi CP/MAS ^{13}C-NMR spectra for macroaggregates under the land management systems studied.

Land management	**Chemical shift regions / ppm**							
	186–220	162–186	142–162	113–142	93–113	61–93	44–61	0–44
	Carbonyl		Aromatic		O-alkyl		OCH_3/NCH	Alkyl
	Ketone & Aldehyde	COO/ N-C=O	Arom. C–O	Arom. C	di-O-alkyl	O-alkyl		
Conventional cropping	1.3	11.8	7.3	20.0	7.7	17.3	11.2	23.4
Cover cropping	1.2	11.2	6.3	17.6	7.7	20.4	11.8	23.8
Natural succession	1.05	10.6	6.3	17.2	7.9	21.9	11.9	23.1

	Alkyl/O-alkyl	Arom-C/O-alkyl	Alkyl + Arom-C/O-alkyl
Conventional cropping	0.94	1.09	2.03
Cover cropping	0.85	0.85	1.70
Natural succession	0.78	0.79	1.56

AAlkyl/O-alkyl, the ratio of the regions 0–44 ppm/64–113 ppm; Arom-C/O-alkyl, the ratio of the regions 113–162 ppm/64–113 ppm; Alkyl + Arom-C/O-alkyl, the ratio of the regions (0–44 ppm+113–162 ppm)/64–113 ppm

Table 5. Correlations between soil organic C (SOC), total N (TN), FTIR derived decomposition indices and $\delta^{15}N$ with intra-aggregate pore characteristics in macroaggregates from the natural succession. Correlation coefficients that were statistically significant at P<0.05 only are listed. Data in bold are significant at P<0.01. The unit for all pores is 'relative fraction', for maximum pore size it is micron and for POM it is cubic micron. The values of FTIR indices and $\delta^{15}N$ are shown in Table S1.

Image-derived pore characteristics	**SOC**	**TN**	**δ^{15}N**	**FTIR decomposition indices**			
				Index 1	**Index 2**	**Index 3**	**Index 4**
	(n=22)			(n=12)			
Total porosity	0.48	0.57	–0.52		–0.66		
Pores <13 µm (image resolution)	0.46	0.57			–0.62		
Image-based porosity (>13 µm)						–0.67	
Pores 13–32 µm				**–0.82**			**–0.81**
Pores 32–58 µm			–0.44				
Pores 58–84 µm							
Pores 84–110 µm							
Pores 110–136			–0.43				
Pores > 136 µm			–0.43		–0.68	–0.58	–0.60
Maximum pore size				–0.66	–0.67	–0.59	–0.67
POM						–0.67	

Index 1: 1648/1423;
Index 2: 1648/1724;
Index 3: 2924/1724;
Index 4: 1630/1510;
$\delta^{15}N$ and all FTIR-based indices increase with increasing degree of OM decomposition;
POM, Particulate OM

Table 6. Results of multiple regression analysis between properties of intra-aggregate OM derived from FTIR indices and δ^{15}N with proportions of large and small pores in the sections of macroaggregates under the natural succession. All values are significant at $\alpha = 0.1$. Bold indicates significance at $\alpha = 0.05$. The values of FTIR indices and δ^{15}N are given in Table S1.

Response variable	**Intercept**	**Regression slopes**		**Coefficient of determination (R^2)**	**Number of samples**
		Large pores (>136 µm)	Small pores (13–32 µm)		
δ^{15}N	3.83	–65.5	–12.5	0.24	22
Index 1	1.65	–16.5	**–6.9**	**0.75**	12
Index 2	1.35	**–17.3**	–1.1	**0.51**	12
Index 3	1.18	–14.9	–1.5	0.41	12
Index 4	1.50	–12.9	**–4.5**	**0.74**	12

Index 1: 1648/1423;
Index 2: 1648/1724;
Index 3: 2924/1724;
Index 4: 1630/1510;
δ^{15}N and all FTIR-based indices increase with increasing degree of OM decomposition

Figure S1. Pore-size distribution for the sections of the macroaggregates studied (*n*=4) from the native succession obtained from X-ray µCT images using 3DMA. The relative pore fractions are obtained from the numbers of medial axis voxels of each size standardized by dividing by the total number of section voxels.

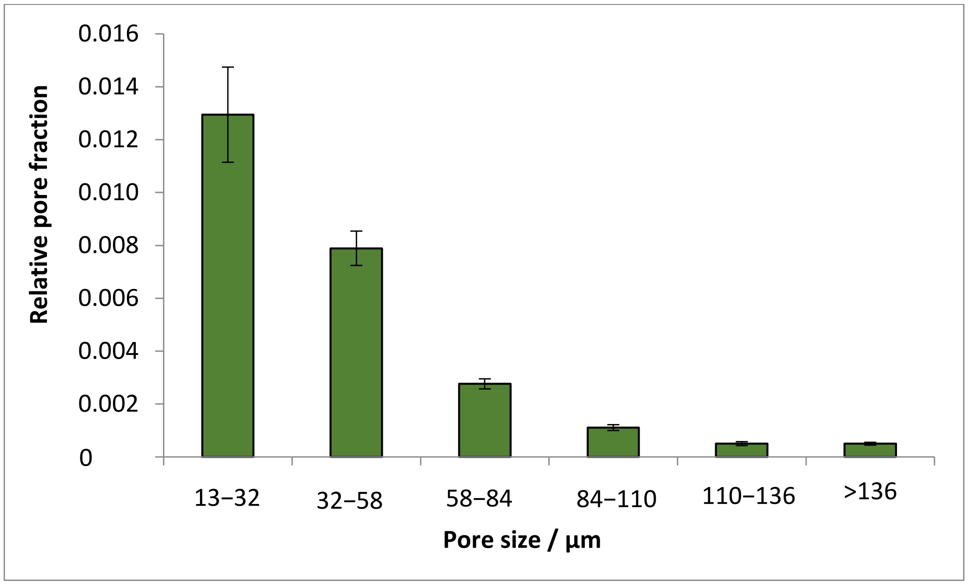

Figure S2. The FTIR spectra for the macroaggregates from conventional cropping, cover cropping and natural succession (n=3).

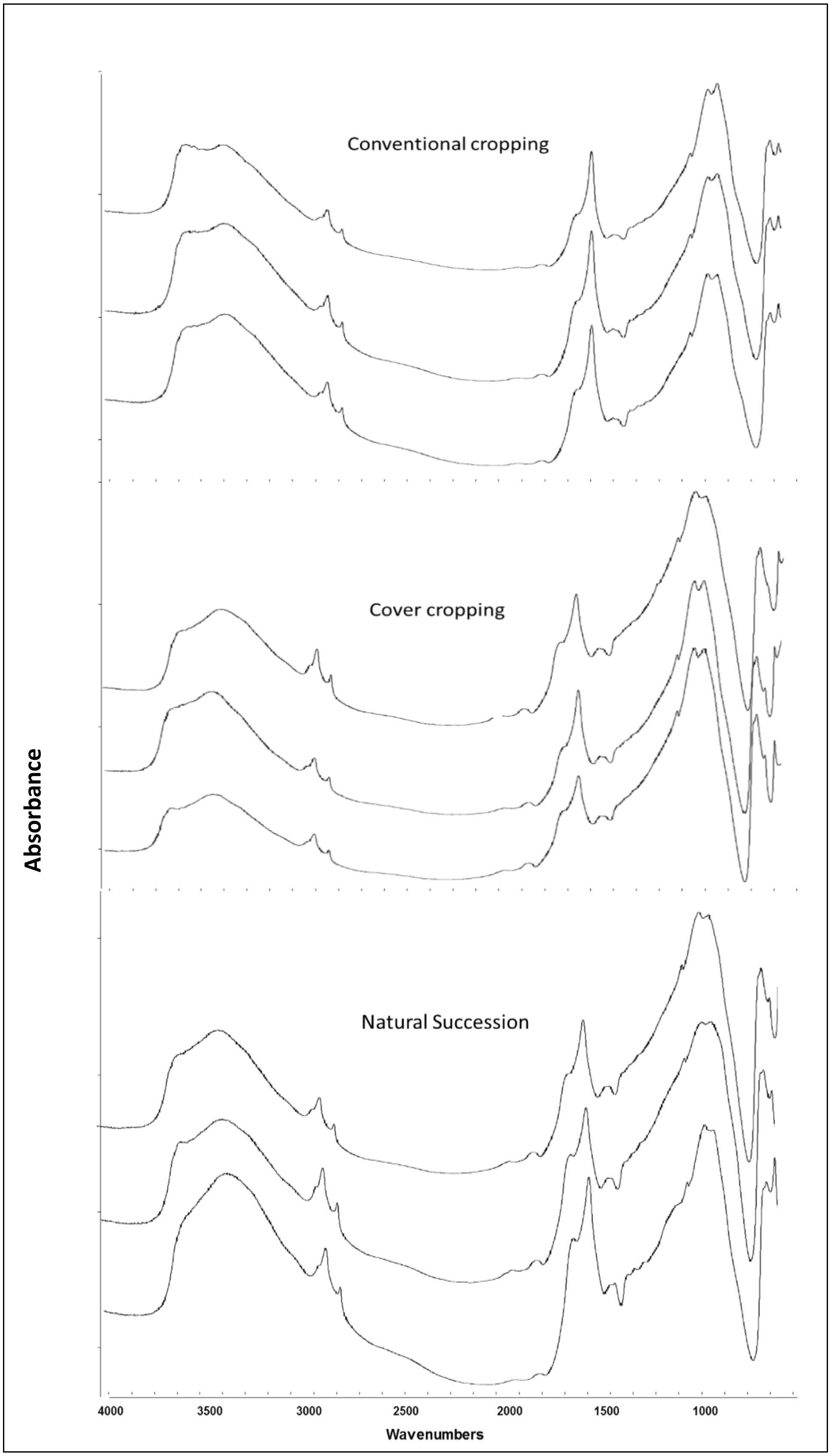

Figure S3. The multi CP/MAS ^{13}C-NMR spectra of macroaggregates from conventional cropping, cover cropping, and natural succession.

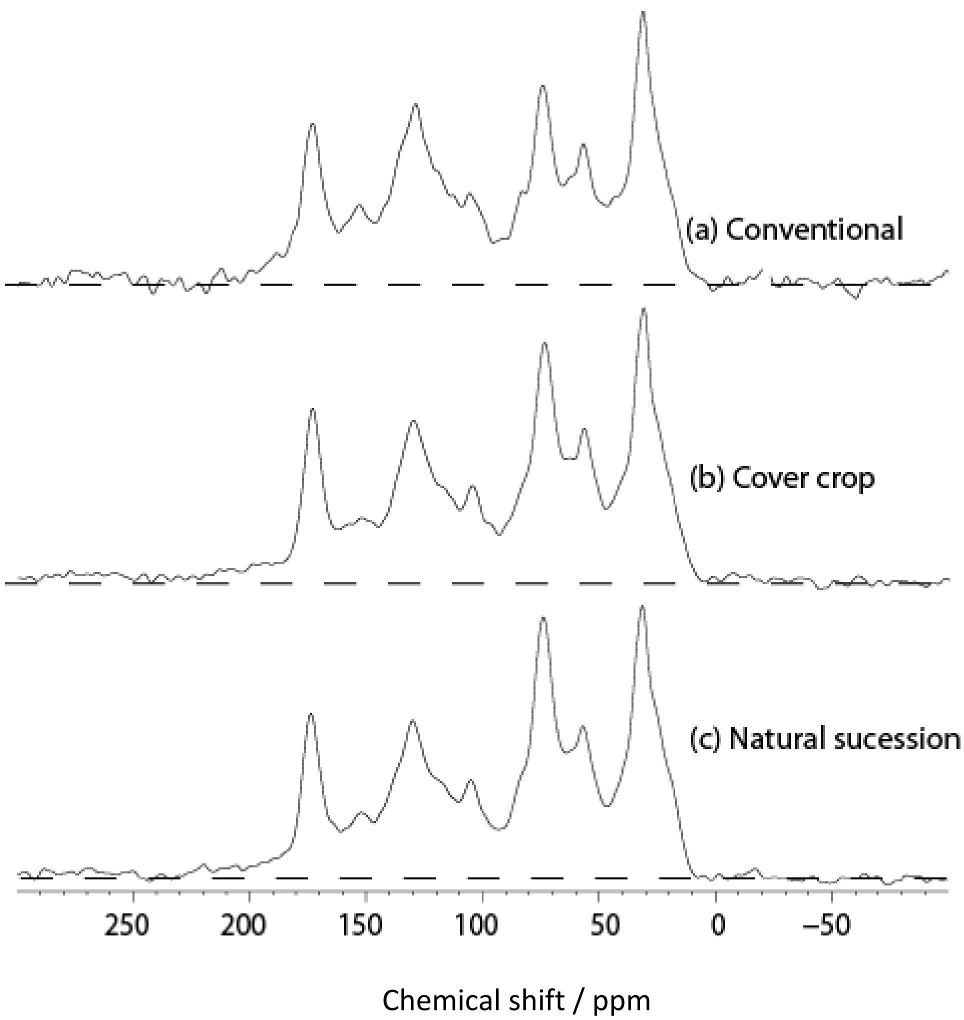

Table S1. Values of FTIR-derived decomposition indices and δ^{13}N for the studied macroaggregate sections (n=12 for FTIR and n=22 for δ^{13}N). The numbers for each section refer to the section ID.

FTIR decomposition indices					δ^{13}N / ‰			
Section	**Index 1**	**Index 2**	**Index 3**	**Index 4**	**Section**	**δ^{13}N**	**Section**	**δ^{13}N**
1	1.40	1.23	1.19	1.32	13	3.27	25	3.35
2	1.16	1.22	0.98	1.17	14	2.21	26	2.94
3	1.27	1.21	1.04	1.24	15	2.65	27	2.96
4	1.51	1.32	1.17	1.41	16	2.15	28	2.54
5	1.37	1.29	1.05	1.31	17	2.14	29	3.80
6	1.31	1.26	1.09	1.27	18	3.35	30	3.81
7	1.34	1.28	1.13	1.29	19	2.78	31	3.54
8	1.40	1.30	1.10	1.35	20	2.79	32	4.05
9	1.38	1.38	1.10	1.34	21	3.36	33	3.98
10	1.21	1.27	1.07	1.23	22	2.40	34	4.41
11	1.50	1.33	1.11	1.40	23	2.67		
12	1.34	1.23	1.07	1.29	24	3.53		

Index 1: 1648/1423;
Index 2: 1648/1724;
Index 3: 2924/1724;
Index 4: 1630/1510;